Conservative and reactive solute transport in constructed wetlands

Steffanie H. Keefe,[1] Larry B. Barber,[1] Robert L. Runkel,[2] Joseph N. Ryan,[3] Diane M. McKnight,[3] and Roland D. Wass[4,5]

Received 7 March 2003; revised 8 August 2003; accepted 17 October 2003; published 27 January 2004.

[1] The transport of bromide, a conservative tracer, and rhodamine WT (RWT), a photodegrading tracer, was evaluated in three wastewater-dependent wetlands near Phoenix, Arizona, using a solute transport model with transient storage. Coupled sodium bromide and RWT tracer tests were performed to establish conservative transport and reactive parameters in constructed wetlands with water losses ranging from (1) relatively impermeable (15%), (2) moderately leaky (45%), and (3) significantly leaky (76%). RWT first-order photolysis rates and sorption coefficients were determined from independent field and laboratory experiments. Individual wetland hydraulic profiles influenced the extent of transient storage interaction in stagnant water areas and consequently RWT removal. Solute mixing and transient storage interaction occurred in the impermeable wetland, resulting in 21% RWT mass loss from main channel and storage zone photolysis (10%) and sorption (11%) reactions. Advection and dispersion governed solute transport in the leaky wetland, limiting RWT photolysis removal (1.2%) and favoring main channel sorption (3.6%). The moderately leaky wetland contained islands parallel to flow, producing channel flow and minimizing RWT losses (1.6%). *INDEX TERMS:* 1890 Hydrology: Wetlands; 1871 Hydrology: Surface water quality; 3230 Mathematical Geophysics: Numerical solutions; *KEYWORDS:* constructed wetlands, OTIS, transient storage

Citation: Keefe, S. H., L. B. Barber, R. L. Kunkel, J. N. Ryan, D. M. McKnight, and R. D. Wass (2004), Conservative and reactive solute transport in constructed wetlands, *Water Resour. Res.*, *40*, W01201, doi:10.1029/2003WR002130.

1. Introduction

[2] Constructed wetlands are increasingly being used to provide supplemental treatment of wastewater treatment plant (WWTP) effluents and to meet wildlife habitat goals. WWTP effluents contain a wide variety of anthropogenic compounds that undergo photolysis, volatilization, biodegradation, and sorption reactions in constructed wetlands. Solutes are transported through primary flow conveying pathways in the main channel of a wetland and temporarily detained in stagnant water areas along the banks, in dense emergent vegetation, and in the subsurface hyporheic zone. For treatment to be more efficient requires a fundamental understanding of the factors that influence solute transport and contaminant removal in both engineered and natural wetlands.

[3] The transport of conservative solutes in constructed wetlands has been classically modeled using plug-flow reactors (PFR) and continuously stirred tank reactors (CSTR), with the system divided into a series of mixed and unmixed regions [*Levenspiel*, 1972]. Several studies have addressed wetland mixing and exchange characteristics with a combination of PFR and CSTR representing main channel transport and storage zone interactions [*Kadlec*, 1994; *Stairs and Moore*, 1994; *Buchberger and Shaw*, 1995; *Werner and Kadlec*, 2000]. *Kadlec* [2000] showed that decay rates are strongly influenced by inlet concentration and hydraulic loading rate (HLR), defined as applied water depth per time [*Kadlec and Knight*, 1996]. *Carleton* [2002] addressed these concerns by linking hydraulics to a Damköhler number distribution function, independent of changes in inlet concentration and accounting for changes in HLR. Other studies have presented complex numerical solutions to simulate discharge and stage depth as a function of wetland properties such as topography and bed resistance [*Feng and Molz*, 1997; *Somes et al.*, 1999], hydrologic inputs including storage [*Guardo and Tomasello*, 1995], and groundwater interactions [*Tisdale and Scarlatos*, 1989]. At the Tres Rios facility [*Wass*, 1997; *Wass, Gerke and Associates, Inc.*, 2001] and other wetland sites [*Rash and Liehr*, 1999; *Stern et al.*, 2001; *Lin et al.*, 2003], tracer testing has been used to quantify bulk hydraulic parameters such as hydraulic retention time (HRT) and mass recovery using spatial and temporal moments, with less effort applied to using tracer test results for reactive solute transport modeling [*Keefe*, 2001].

[4] In this report we evaluate bromide transport and rhodamine WT (RWT) transport, photolysis, and sorption in three separate wetlands at the City of Phoenix, Arizona, Tres Rios Demonstration Wetland Facility [*Wass*, 1997; *Wass, Gerke and Associates, Inc.*, 2001]. On the basis of site and design criteria, the wetland water losses range from relatively impermeable, to moderately leaky, to significantly leaky. The wetlands also vary in island placement, vegeta-

[1]U.S. Geological Survey, Boulder, Colorado, USA.
[2]U.S. Geological Survey, Denver, Colorado, USA.
[3]Department of Civil and Environmental Engineering, University of Colorado, Boulder, Boulder, Colorado, USA.
[4]Water Services Department, Phoenix, Arizona, USA.
[5]Now at Wass, Gerke and Associates, Inc., Tempe, Arizona, USA.

0043-1397/04/2003WR002130$09.00

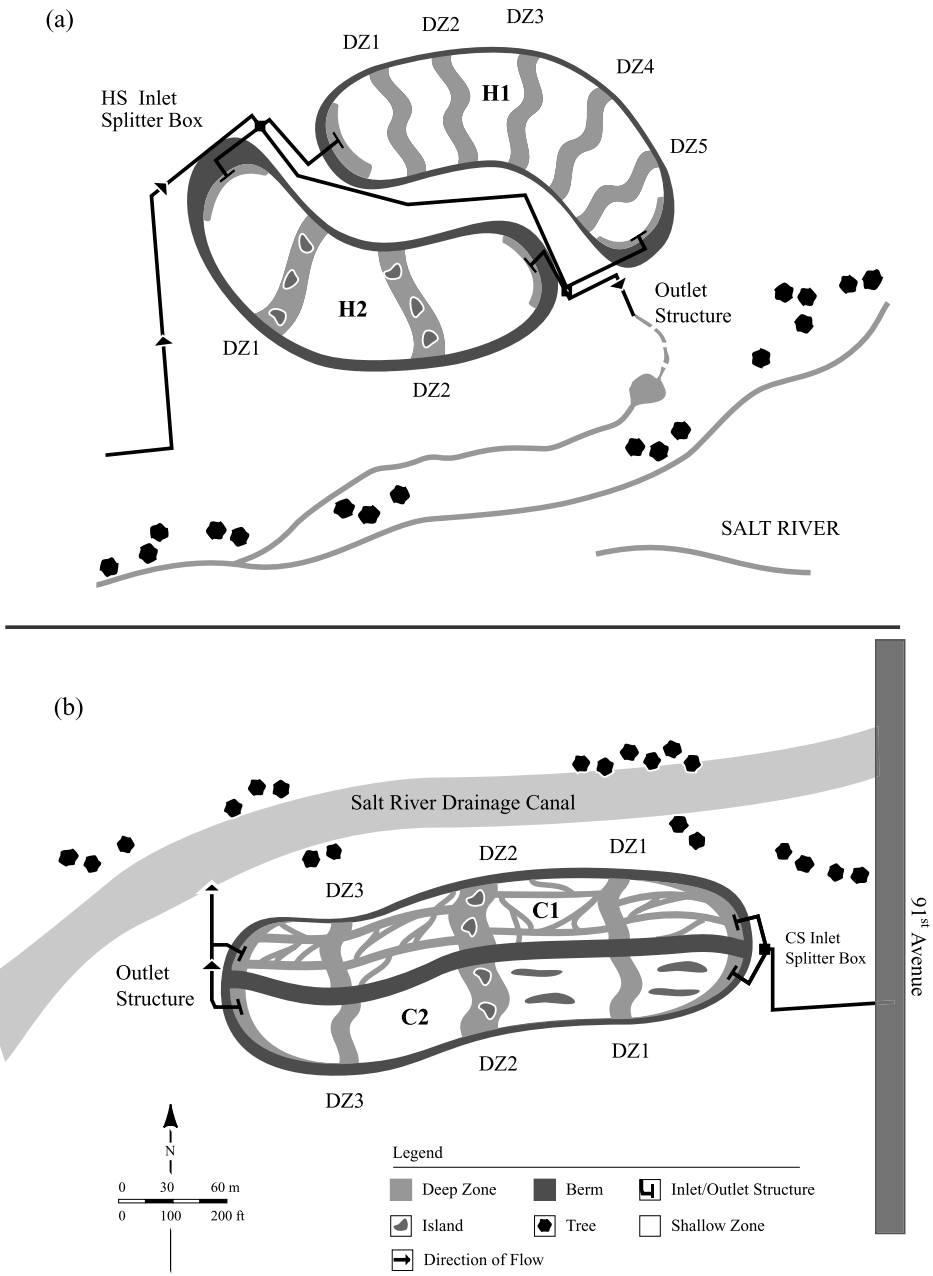

Figure 1. Tres Rios Demonstration Wetlands, Phoenix, Arizona, site maps: (a) Hayfield and (b) Cobble. Legend is H1, Hayfield 1 wetland; H2, Hayfield 2 wetland; C1, Cobble 1 wetland; C2, Cobble 2 wetland; DZ, deep zone; HS, Hayfield site; CS, Cobble site. Arrows show direction of flow.

tion coverage, and internal deep zone configuration. Sodium bromide, a conservative tracer, was used to quantify wetland hydrodynamics describing main channel solute transport and interaction with transient storage areas. Rhodamine WT ($C_{29}H_{29}N_2O_5Na_2Cl$) was used as a representative reactive organic solute that undergoes first-order photolysis [*Smart and Laidlaw*, 1977; *Tai and Rathbun*, 1988; *Suijlen and Buyse*, 1994; *Getsinger et al.*, 1997] and sorption [*Bencala et al.*, 1983; *Sabatini and Austin*, 1991; *Ptak and Schmid*, 1996; *Kasnavia et al.*, 1999; *Vasudevan et al.*, 2001; *Sutton et al.*, 2001]. The reactive processes were quantified with respect to the hydrologic characteristics of each wetland, and the amount of removal in the active channel and stagnant water areas was determined. The ability to simulate conservative transport, first-order decay reactions, and sorption processes provides a framework for investigating additional processes in constructed wetlands.

[5] The objective of this study was to simulate solute transport and chemical reactions in a forward, predictive manner using a comprehensive and transferable methodology to analyze tracer test data. The approach reported here uses a numerical model to solve a one-dimensional advection-dispersion equation with transient storage to establish hydraulic transport characteristics. The wetland is subdivided into a series of small, well-mixed segments where a solute undergoes first-order removal, kinetic sorption, and exchange with transient storage areas. The model provides a means of quantifying transport and reaction processes based

on field experiments, laboratory measurements, fundamental chemical principles, and data reported in the literature.

[6] The physical interpretation of transport parameters is discussed for a range of wetland configurations and hydraulic profiles. The reactive RWT simulations established the relative amount of mass loss due to each removal process (photolysis and sorption). First-order RWT photolysis rates were defined by solar radiation measurements and compound light absorption properties. Sorption to wetland solids was quantified from sorption isotherm experimental data, and then the reactive parameters were evaluated as a function of wetland hydrodynamics. These simulations present a means of quantifying physical and chemical processes and are introduced as a technique for investigating reactive transport in constructed wetlands.

2. Methods

2.1. Site Description

[7] The Tres Rios Demonstration Wetland facility consists of the Cobble and Hayfield systems, each having a paired set of wetlands with alternating shallow and deep zones (Figure 1). The open-water, deep zones are 1 m deeper than the shallow zones containing emergent vegetation including soft-stem bulrush (*Schoenoplectus tabernaemontani*) and Olney's bulrush (*Schoenoplectus americanus*). All of the wetlands have controlled flow through 60° V-notch inlet weirs and outlet headboards. The four wetlands receive nearly 7500 m^3 d^{-1} (two million gallons per day) of secondary treated, denitrified, chlorinated/dechlorinated wastewater discharged from the 91st Avenue WWTP [*Whitmer*, 1998].

[8] The two Hayfield wetlands (H1 and H2) were constructed on a former agricultural field consisting of a topsoil that curtails groundwater seepage [*Wass, Gerke and Associates, Inc.*, 2001]. The H1 wetland has five internal deep segments, which alternate with six shallow-water zones, situated perpendicular to the main-flow pathway. In June 1999, the H1 wetland contained ~30% dense bulrush growing in the shallow areas as well as duckweed (*Lemna spp.*) growth on the water surface (Table 1) and the HLR was 15 cm d^{-1}. The H2 wetland has two internal deep zones with islands and three shallow zones.

[9] The Cobble wetlands (C1 and C2) were built on the Salt River alluvium, a coarse sediment that allows significant leakage [*Wass, Gerke and Associates, Inc.*, 2001]. The unlined C1 cell contains deep zones oriented both parallel and perpendicular to the direction of flow. In the summer of 1999, the C1 wetland contained ~5% bulrush at the inlet and along the sides of the wetland, an extensive duckweed cover (Table 1), and the HLR was 25 cm d^{-1}. The C2 wetland was lined with loamy topsoil to curtail water losses and had elongated islands in two shallow zones and the center deep zone. During the field survey, the C2 wetland had ~25% emergent vegetation concentrated in the first and second shallow zones with minimal vegetative cover near the outlet (Table 1), and the HLR was 15 cm d^{-1}.

2.2. Field Tracer Test

[10] Coupled sodium bromide and RWT tracer tests were conducted in the H1, C1, and C2 wetlands. Sodium bromide (reagent grade, Alameda Chemical) and RWT (20 wt % aqueous solution, Crompton and Knowles Corp.) were mixed together in a 55 gallon polyethylene barrel containing influent water until completely dissolved, and then pumped into the inlet splitter box. The tracer plume was discharged into the wetland through a subsurface pipe that introduces effluent laterally across the inlet deep zone, transverse to the direction of flow. The tracer injectate concentrations and injection times are listed in Table 1.

Table 1. Wetland Basin Configurations, Average Water Budget, Upstream Boundary Conditions, and Injection Times During the H1, C1, and C2 Tracer Tests, 24 June Through 6 July 1999[a]

	H1 Wetland	C1 Wetland	C2 Wetland
Basin length, m	228	275	275
Basin width, m	60	35	35
Surface area, ha	1.2	0.9	0.9
Number of deep zones	5	4	4
Number of shallow zones	6	5	5
Shallow zone depth, cm	30	45	45
HLR, cm d^{-1}	15	25	15
Bulrush coverage, %	30	5	25
A_{design}, m^2	35.2	36.0	24.0
Q_{in}, m^3 d^{-1}	1890	2310	1440
Q_{out}, m^3 d^{-1}	1470	477	707
Q_{Et}, m^3 d^{-1}	131	89	88
$Q_{seepage}$, m^3 d^{-1}	289	1740	645
Volume, m^3	6840	6720	4780
nHRT, days	3.62	2.91	3.32
$C_{bc,br}$, mg L^{-1}	7760	7530	9610
$C_{bc,RWT}$, mg L^{-1}	225	77.8	139
Injection time, min	7.53	8.00	8.17

[a]HLR, hydraulic loading rate; A_{design}, average design cross-sectional area; Q_{in}, average daily inflow; Q_{out}, average daily outflow; Q_{Et}, average daily evapotranspiration losses; $Q_{seepage}$, average daily infiltration losses; nHRT, nominal hydraulic retention time; $C_{bc,br}$, concentration of bromide at upstream boundary condition; and $C_{bc,RWT}$, concentration of RWT at upstream boundary condition.

[11] Prior to the start of the tracer tests, baseline water samples were collected in 1 L amber glass bottles at each inlet and outlet location. During each tracer test, water samples were collected every hour by an autosampler (American Sigma, model 1350) at the wetland outlet for the first 2 weeks and every 4–6 hours at the end of the experiment. Samples were retrieved daily, split into amber polyethylene bottles for separate analysis, and stored at room temperature. Bromide concentrations were determined by ion chromatography [*Pfaff et al.*, 1997]. RWT was analyzed using a Turner model 10A fluorometer (G4T5 clear quartz lamp, 546 nm excitation filter, >570 nm emission filter, >535 nm reference filter). A standard curve ranging from 0.1 to 1000 μg L^{-1} was developed from RWT stock solution to determine concentrations in field samples.

3. Solute Transport Modeling

[12] Physical and chemical processes governing solute transport in the Tres Rios wetlands were quantified using tracer test data and the one-dimensional transport with inflow and storage (OTIS) numerical solute transport model (http://co.water.usgs.gov/otis) [*Runkel*, 1998]. OTIS has been used extensively in stream and river systems [*Bencala*, 1983; *Valett et al.*, 1996; *Morrice et al.*, 1997; *Harvey and Fuller*, 1998; *Runkel et al.*, 1998; *Chapra and Wilcock*, 2000; *Fernald et al.*, 2001; *Laenen and Bencala*, 2001; *McKnight et al.*, 2001].

[13] Because of the elongated shape of the constructed wetlands (aspect ratios, length/width, of 3.8 for H1 and 7.9 for C1 and C2, Table 1), each wetland was modeled as a one-dimensional system with advection acting only in the longitudinal direction. One-dimensional models of solute transport typically consist of an advective term to describe bulk transport in the downstream direction and a dispersion term to describe mixing due to variations in the velocity field. In the case of the Tres Rios wetlands, dispersive mixing does not adequately describe the observed spreading of solutes, as some of the tracer is detained in stagnant water areas. The failure of the one-dimensional advection-dispersion equation to describe solute mixing has been widely noted in the literature for stream systems, and alternate models that include the process of transient storage have been developed [*Bencala and Walters*, 1983]. Use of the transient storage model represents a compromise between a strictly one-dimensional approach and a two-dimensional model, and is quasi-two-dimensional, with the storage zone representing the second dimension [*Runkel and Chapra*, 1993].

[14] Each wetland is conceptually divided into two areas: the main channel and the storage zone. The main channel represents areas of the wetland in which advection is the dominant transport mechanism. In addition to advection, physical processes influencing solute concentrations in the main channel include dispersion and exchange with the storage zone. Chemical processes considered in the main channel include first-order photolysis and sorption. The storage zone represents stagnant water areas (e.g., quiescent pools surrounded by emergent vegetation) and the hyporheic zone underlying the wetland. Physical and chemical processes considered in the storage zone include exchange with the main channel, first-order photolysis, and sorption. Governing equations for the main channel and transient storage zone are [*Runkel*, 1998]

$$\frac{\partial C}{\partial t} = -\frac{Q}{A}\frac{\partial C}{\partial x} + \frac{1}{A}\frac{\partial}{\partial x}\left(AD\frac{\partial C}{\partial x}\right) + \frac{q_{evap}}{A}(C) + \alpha(C_S - C) - k \quad C + \rho \quad k_{sorp}(C_{solid} - K_d C) \tag{1}$$

$$\frac{dC_S}{dt} = \alpha\frac{A}{A_s}(C - C_S) - k_{stor}C_S + k_{sorp,stor}\left(\hat{C}_S - C_S\right) \tag{2}$$

where C and C_S are concentrations in the main channel and storage zones (mg L^{-1} for bromide; μg L^{-1} for RWT), x is distance (m), t is time (s), Q is volumetric flow rate (m^3 s^{-1}), q_{evap} is rate of evaporation (m^3 s^{-1} m^{-1}), D is longitudinal dispersion coefficient (m^2 s^{-1}), A is main channel cross-sectional area (m^2), α is storage zone exchange coefficient (s^{-1}), k is main channel direct photolysis rate coefficient (s^{-1}), C_{solid} is sorbed concentration on the solid (μg kg^{-1}), K_d is solid-water distribution coefficient (L μg^{-1}), k_{sorp} is main channel sorption rate coefficient (s^{-1}), ρ is mass of accessible solid available for sorption/volume water (μg L^{-1}), A_s is storage zone cross-sectional area (m^2), $\hat{C}_s$ is equilibrium background storage zone concentration (μg L^{-1}), k_{stor} is storage zone direct photolysis rate coefficient (s^{-1}), and $k_{sorp,stor}$ is storage zone sorption rate coefficient (s^{-1}).

[15] Application of equations (1) and (2) requires specification of an upstream boundary condition in terms of the tracer concentration at the wetland inlet. The upstream boundary concentration was set equal to effluent concentration for all times before and after the tracer addition. During tracer addition, the boundary concentration was set equal to the concentration that would result from mixing of effluent with the injected tracer. The distance required for complete transverse mixing of the tracer plume (0.6–2.8 m) was <1% of the total travel length of each wetland due to the subsurface input pipe that introduces tracer perpendicular to the direction of flow.

[16] Because of the spatial variability in wetland morphology, the extent of open water areas and emergent vegetation zones varies along the length of each wetland. Measurement of average cross-sectional area would require numerous transects to obtain representative values. As with tracer studies in stream systems, main channel and storage zone cross-sectional areas for each wetland were estimated from tracer concentrations at a reach endpoint (i.e., the wetland outlet) and represent values integrated over the length of the wetland. The design cross-sectional areas, A_{design}, were calculated based on a representative trapezoidal channel with an average water depth of 0.5 m, a side slope of 3:1, and wetland width independent of emergent vegetation coverage (Table 1).

[17] Quasi-steady state flow exists in the wetlands where discharge and water depth are constant with time at one location but change along the length of the wetland. For reactive solutes, exchange with the storage zone at steady state influences mass balance with active photolytic and sorption reactions in stagnant water areas affecting solute concentrations. Each wetland was modeled as a single reach with multiple well-mixed segments, where the segment length was set to 1 m to minimize errors in the finite difference approximations of the spatial derivatives in equation (1) [*Runkel and Chapra*, 1993]. Flow losses due to seepage and evaporation were differentiated using evaporation data from the Litchfield weather gauging station (http://ag.arizona.edu/azmet). Reference evapotranspiration measurements were converted to evaporative volumetric flow rate, Q_{Et} values based on a continuously saturated crop-coefficient and normalized to the surface area of each wetland [*Wass, Gerke and Associates, Inc.*, 2001]. The Q_{Et} and groundwater seepage volumetric flow rate, $Q_{seepage}$ terms (Table 1) are divided by the wetland length to obtain q_{evap} and $q_{seepage}$ (equation (1)), with units that are consistent with OTIS inflow/outflow terms. The volumetric flow rate in each stream segment, $Q(x)$, was set by considering the observed loss of flow between the inlet and outlet weir (Table 1):

$$Q(x) = Q_{in} - q_{evap}\,x - q_{seepage}\,x \tag{3}$$

Volumetric nominal hydraulic retention times (nHRT) are reported in Table 1 as the ratio of the wetland design volume and the total inflow (volume/Q_{in}).

3.1. Conservative Transport (Bromide)

[18] Bromide is considered a conservative tracer that does not undergo sorption or chemical and biological transformations. The bromide tracer test response curves were therefore used to quantify physical processes affecting solute transport in each wetland. As with most applications of the transient storage approach, the physical parameters in equations (1) and (2) (A, A_s, α, and D) were estimated by

Table 2. Estimation Techniques for Conservative Transport Parameters (D, Longitudinal Dispersion Coefficient; A, Main Channel Cross-Sectional Area; A_s, Storage Zone Cross-Sectional Area; α, Storage Zone Exchange Coefficient), and Reactive Parameters for Photolysis (k, Main Channel Direct Photolysis Rate Coefficient; k_{stor}, Storage Zone Direct Photolysis Rate Coefficient) and Sorption (K_d, Solid-Water Distribution Coefficient; ρ, Mass of Accessible Sorbent/Volume Water; k_{sorp}, Main Channel Sorption Rate Coefficient; $k_{sorp,stor}$, Storage Zone Sorption Rate Coefficient)[a]

Parameter	Units	Estimation Technique	Data Set
D	$m^2\ s^{-1}$	numerical optimization	bromide tracer test
A	m^2	numerical optimization	bromide tracer test
A_s	m^2	numerical optimization	bromide tracer test
α	s^{-1}	numerical optimization	bromide tracer test
k	s^{-1}	calculation	field measured W_λ and lab measured ε_λ and α_λ
k_{stor}	s^{-1}	calculation	field measured W_λ and lab measured ε_λ and α_λ
K_d	$L\ \mu g^{-1}$	calculation	lab measured $K_{d,sed}$ and $K_{d,det}$; literature-based $K_{d,veg}$
ρ	$\mu g\ L^{-1}$	numerical optimization	RWT tracer test
k_{sorp}	s^{-1}	numerical optimization	RWT tracer test
$k_{sorp,stor}$	s^{-1}	numerical optimization	RWT tracer test

[a] W_λ, total light intensity at wavelength λ; ε_λ, molar extinction coefficient at wavelength λ; α_λ, beam attenuation coefficient at wavelength λ; $K_{d,sed}$, sediment-water distribution coefficient; $K_{d,det}$, detritus-water distribution coefficient; and $K_{d,veg}$, vegetation-water distribution coefficient.

solving the transport equation using the experimental data. A series of model simulations were conducted with physical parameter estimates to determine values that produced correspondence between simulated and observed concentrations. This parameter estimation process was facilitated by OTIS-P, which uses a nonlinear least squares approach to minimize the differences between simulated and observed solute concentration [*Runkel*, 1998], providing an objective means of parameter estimation as well as a measure of the uncertainty (e.g., standard deviation) associated with each estimate. The average HRT is reported as the center of mass of each tracer response curve.

3.2. Reactive Transport (RWT)

[19] Constructed wetlands provide large, shallow open-water areas fully exposed to incident solar radiation that are ideal for photolysis reactions. Transport within a wetland system results in contact between water and solid surfaces (sediment, vegetation, detritus) that promote sorption reactions. Reactive simulations were therefore conducted to quantify the effects of photolysis and sorption reactions on RWT transport, using the physical parameters estimated from bromide data and chemical parameters discussed below. Table 2 details the estimation techniques and corresponding data sets used for each parameter of the conservative and reactive simulations.

3.2.1. Direct Photolysis

[20] Photolysis was modeled as a first-order degradation process with rate coefficients specified for both the main channel (k, equation (1)) and storage zone (k_{stor}, equation (2)). The photolysis rate coefficient is [*Schwarzenbach et al.*, 1993]

$$k = \Phi_r k_a = \Phi_r \Sigma k^{\circ}_{a,\lambda} S_\lambda = \Phi_r \Sigma (2.3\ W_\lambda D_\lambda \varepsilon_\lambda) S_\lambda \qquad (4)$$

where Φ_r is reaction quantum yield (mol einstein^{-1}) and k_a is specific rate of light absorption (einstein mol^{-1} s^{-1}). The quantum yield is defined as the ratio of the number of molecules that photoreact to the number of quanta absorbed by the system [*U.S. Environmental Protection Agency* (*U.S. EPA*), 1998] and is set to 1.82×10^{-7} moles einstein^{-1} [*Tai and Rathbun*, 1988]. The k_a parameter is defined as the distribution of the rate of light absorption at the surface at wavelength λ ($k_{a,\lambda}{}^o$ in einstein mol^{-1} s^{-1}), throughout a well-mixed water column quantified by a dimensionless light screening factor at wavelength λ (S_λ). The $k_{a,\lambda}{}^o$ parameter encompasses the total light intensity at wavelength λ (W_λ, in einstein cm^{-2} s^{-1}), the dimensionless near-surface distribution function at wavelength λ (D_λ), and the molar extinction coefficient at wavelength λ (ε_λ in L mol^{-1} cm^{-1}). The D_λ value estimates solar flux penetration into a well-mixed water column and is set equal to 1.2 for nonturbid waters [*Zepp and Cline*, 1977].

[21] The S_λ parameter quantifies the decrease in light absorption by the compound of interest as a function of depth of the well-mixed water layer (z_{mix}, in cm) due to diminished sunlight penetration and the presence of additional light-absorbing compounds [*Schwarzenbach et al.*, 1993]:

$$S_\lambda = \frac{[1 - 10^{-D_\lambda \alpha_\lambda z_{mix}}]}{2.303\, D_\lambda\, z_{mix}\, \alpha_\lambda} \qquad (5)$$

where α_λ is beam attenuation coefficient at wavelength λ (cm^{-1}). The ε_λ parameter describes the fraction of absorbance due to the compound of interest, and the α_λ term quantifies the fraction of background light-absorbing compounds present in the environmental sample.

3.2.2. Sorption

[22] Sorption of RWT was modeled using the kinetic mass transfer approach presented by *Bencala* [1983] as implemented in equations (1) and (2). In this approach, main channel sorption is modeled using K_d, ρ, k_{sorp}, and $k_{stor,sorp}$ parameters. Because of the variety of solid surfaces present in the Tres Rios wetlands (sediment, vegetation, detritus), the solid-water distribution coefficient was estimated using a weighted average:

$$K_d = f_{sed} K_{d,sed} + f_{det} K_{d,det} + f_{veg} K_{d,veg} \qquad (6)$$

where f_{sed} is fraction of sorptive sediment, $K_{d,sed}$ is sediment-water distribution coefficient (L μg^{-1}), f_{det} is fraction of sorptive detritus, $K_{d,det}$ is detritus-water distribution coefficient (L μg^{-1}), f_{veg} is fraction of sorptive

vegetation, and $K_{d,veg}$ is vegetation-water distribution coefficient (L μg^{-1}). The ρ, k_{sorp}, and $k_{stor,sorp}$ parameters were determined by solving transport equations (1) and (2) using the RWT experimental data facilitated by the OTIS-P estimation algorithm.

4. Results

4.1. Conservative Transport (Bromide)

[23] Figure 2 depicts field measurements and model simulation results for the H1, C1, and C2 bromide tracer experiments. The H1 simulation reproduced the observed bromide peak as well as the rising and falling limbs of the field tracer response curve (Figure 2a), and the mass recovery and HRT values differed by less than 1% from field concentrations (Table 3). Simulation of the C1 and C2 bromide tracer response curves (Figures 2b and 2c) also demonstrated general agreement with the rising and falling limbs as well as the peak field concentration, although not as good as for H1. The C1 simulation did not precisely replicate the tailing behavior of field measurements after 170 hours with a 1.4% greater mass recovery and 15% longer HRT than field observations. The C2 simulation deviated from the falling limb of the field tracer response curve between 65 and 150 hours and had a 7% lower mass recovery and 3.4% shorter HRT than determined from field concentrations. Volumetric nominal hydraulic retention times (nHRT, Table 1) differ by 7.44–27.4 hours (8–47%) from tracer test based HRT values. Overall, 8–15% (Table 3) of the bromide mass was not recovered at the wetland outlet (after correcting for groundwater seepage) due in part to the timescale of the tracer test, which may have been shorter than the time needed for complete recovery of the tracer cloud.

[24] Physical transport parameters for each wetland are reported in Table 3. The standard deviation for each parameter is reported as an estimate of uncertainty. These transport parameters are used to calculate the fraction of total reach volume occupied by the storage zone, F_{mean} ($A/A + A_s$), and the fraction of the median travel time attributable to transient storage, F_{med} (quantified by the median travel time due to advection-dispersion and transient storage relative to the median travel time due solely to advection-dispersion), as described by *Runkel* [2002]. Dispersion coefficients are presented for the OTIS-P analysis (D) and independent moments analysis ($D_{moments}$) with both estimates falling within the eddy diffusion range of horizontal surface waters [*U.S. EPA*, 1985]. The Reynolds numbers, R_e, and Froude numbers, F_r, designate laminar and subcritical flow for all wetlands studied [*Chaudhry*, 1993]. The Peclet numbers, P_e, indicate that the wetlands have transitional flow between a PFR and CSTR [*Chapra*, 1997].

[25] Analysis of the H1 tracer test results indicates the bromide solute plume undergoes mixing in the internal deep zones positioned perpendicular to flow, as well as in temporary storage in stagnant water areas. The A parameter was 69% of the A_{design} value corresponding to ~30% emergent vegetation in the H1 wetland. Standard deviations of the A, D, and A_s parameters were within 7% of mean values while the α term was more uncertain (standard deviation was 15% of the mean). The storage zone occupied 14% of the total reach volume (F_{mean}) and accounted for 6.5% of the total median travel time (F_{med}).

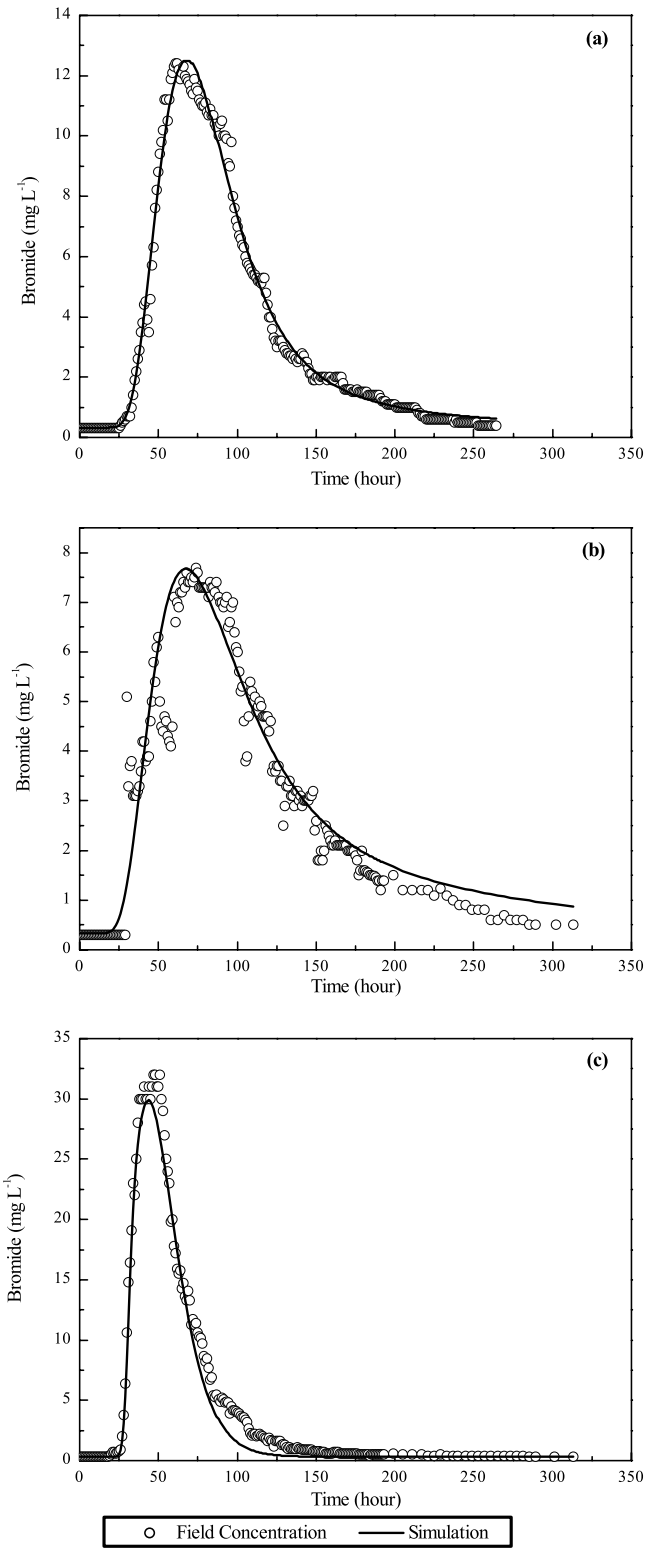

Figure 2. Bromide tracer test field data and transport simulations for the (a) Hayfield 1, (b) Cobble 1, and (c) Cobble 2 wetlands, 24 June through 6 July 1999.

Table 3. Conservative Transport Parameters and Associated Standard Deviations, Median Travel Time due to Transient Storage (F_{med}), Mean Travel Time due to Transient Storage (F_{mean}), and Average Velocity (u_{avg}) for the H1, C1, and C2 Wetland Bromide Tracer Test Simulations[a]

Parameter	H1 Wetland	C1 Wetland	C2 Wetland
D, $m^2\ s^{-1}$	9.97×10^{-3} ($\pm 2.35 \times 10^{-4}$)	2.13×10^{-2} ($\pm 4.01 \times 10^{-4}$)	2.53×10^{-3} ($\pm 7.75 \times 10^{-4}$)
A, m^2	24.19 (±0.21)	18.07 (±0.13)	5.20 (±0.15)
A_s, m^2	3.90 (±0.26)	...	3.06 (±0.15)
α, s^{-1}	9.00×10^{-7} ($\pm 1.35 \times 10^{-7}$)	...	2.78×10^{-5} ($\pm 3.10 \times 10^{-6}$)
F_{med}, %	6.46	...	33.7
F_{mean}, %	13.9	...	37.1
u_{avg}, $m\ d^{-1}$	71.4	77.5	204
Mass recovery,[b] %	70	16	46
Hydraulic retention time,[b] days	3.89	4.01	2.43
Variance about the mean,[b] $days^2$	3.13	4.21	2.06
Moments dispersion ($D_{moments}$),[b] $m^2\ s^{-1}$	1.44×10^{-2}	1.18×10^{-2}	9.69×10^{-2}
Peclet number, P_e[b]	8.53	6.48	4.48
Reynolds number, R_e[c]	401	554	425
Froude number, F_r[c]	2.31×10^{-4}	2.94×10^{-4}	9.35×10^{-4}

[a] D, longitudinal dispersion coefficient; A, main channel cross-sectional area; A_s, storage zone cross-sectional area; α, storage zone exchange coefficient.
[b] Mass recovery, hydraulic retention time, variance about the mean, moments dispersion coefficient, and Peclet number values were obtained using methods from *Kadlec* [1994].
[c] Reynolds and Froude numbers were obtained using methods from *Chaudhry* [1993].

[26] The leaky nature of the C1 sediments allowed large (76%) permanent losses of water and associated solutes, and dominated the hydraulics of the wetland. Simulation results established that advection and dispersion governed transport while transient storage did not significantly affect bromide outlet concentrations. The A parameter was 50% of the A_{design} value, indicating the main transport channel of the solute plume was half of the C1 design criteria. The standard deviation of the A and D parameters fell within 2% of the mean values.

[27] Bromide transport in the C2 wetland was characterized by channel flow due to island placement. The average flow velocity in the C2 wetland was 62–65% faster than the H1 and C1 wetlands, and the A parameter was 22% of the A_{design} value. The standard deviation of the A and A_s terms were within 5% of the mean, whereas the α and D parameters had more uncertainty, with standard deviations of 11% and 31% of the mean. The large contribution of transient storage to reach volume (F_{mean} = 37%) and travel time (F_{med} = 34%) may be attributed to the lateral spreading associated with the islands. The two-dimensional nature of solute transport in the C2 wetland is reflected in the size and significance of the storage zone.

4.2. Reactive Transport (Rhodamine WT)

[28] A forward, predictive simulation was performed for each RWT tracer test using independently calculated photolysis rates (k, k_{stor}) and transport parameters established from the bromide tracer test simulations (A, A_s, D, α). A second approach incorporated both photolysis and sorption removal pathways by fixing an experimentally determined weighted distribution coefficient (K_d) and estimating the reactive sorption parameters (ρ, k_{sorp}, $k_{sorp,stor}$) using the nonlinear least squares approach in OTIS-P (Table 4). The equilibrium background storage zone concentration ($\hat{C}_s$) was set to the background fluorescence, which was equivalent to 0.45 $\mu g\ L^{-1}$ RWT.

4.2.1. Photolysis

[29] An estimate of W_λ (equation (4)) was calculated from solar intensity measurements (LiCor model 1800UW spectroradiometer) over a λ range from 300 to 850 nm on 23 June 1999 (Figure 3a). Spectral irradiance was recorded eight times from 7:00 A.M. to 5:00 P.M. in direct sunlight and once in the shade. Shade measurements represent sunlight exposure in densely vegetated areas designated as storage zones. Solar intensity data were authenticated with measurements from the Litchfield weather station. The ε_λ parameter was measured using a Hewlett-Packard model 8453 photodiode array spectrophotometer to quantify the absorbance of RWT and the H1 influent at 1 nm intervals over a λ range from 300 to 850 nm. The α_λ parameter (equation (5)) was estimated from absorbance measurements of the H1 influent to quantify the fraction of absorbance due to background light-absorbing constituents.

Table 4. Reactive Transport OTIS Output Parameters for the H1, C1, and C2 Wetland RWT Tracer Test Simulations[a]

Parameter	H1 Wetland	C1 Wetland	C2 Wetland
ρ, $\mu g\ L^{-1}$	329 (±13.3)	3210 (±1803)	928 (±92.5)
k_{sorp}, s^{-1}	5.89×10^{-6} ($\pm 3.31 \times 10^{-7}$)	2.92×10^{-7} ($\pm 1.77 \times 10^{-7}$)	3.46×10^{-6} ($\pm 3.73 \times 10^{-7}$)
$k_{sorp,stor}$, s^{-1}	1.49×10^{-5} ($\pm 2.26 \times 10^{-6}$)	...	...
Mass recovery,[b] %	49	12	37
Hydraulic retention time,[b] days	4.05	4.17	2.70
Variance about the mean,[b] $days^2$	4.68	5.04	2.89

[a] Parameters are ρ, mass of accessible sorbent/volume water; k_{sorp}, main channel sorption rate coefficient; and $k_{sorp,stor}$, storage zone sorption rate coefficient. Standard deviations are reported in parentheses.
[b] Mass recovery, hydraulic retention time, and variance about the mean values obtained using methods from *Kadlec* [1994].

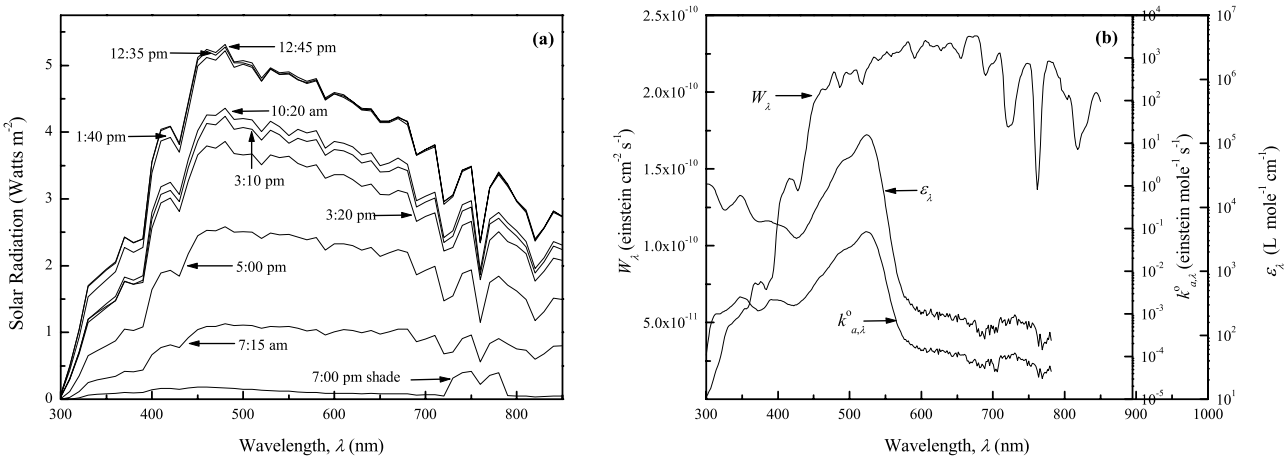

Figure 3. (a) Light intensity distribution, W_λ, and (b) molar extinction coefficient, ε_λ, and near-surface specific rate of light absorption, $k^o_{a,\lambda}$, for RWT at 12:45 P.M., peak solar flux on 23 June 1999 at the Tres Rios Demonstration wetlands.

Additional absorbance measurements were conducted on distilled water spiked with 1 mg L^{-1} RWT to quantify the fraction of absorbance due specifically to the RWT molecule (ε_λ). The z_{mix} parameter was set to 0.5 m, the average depth of the H1 wetland during the field experiments. Figure 3b depicts the $k^o_{a,\lambda}$ value (equation (4)) for RWT near the peak solar flux at the Tres Rios wetlands site. The product of ε_λ and W_λ outlines the wavelength range where the wetland basins phototransform RWT, and the resulting $k^o_{a,\lambda}$ curve approximates the photodecay rate at the water surface. The area under the $k^o_{a,\lambda}$ curve represents the total near-surface specific absorption rate, k^o_a, of RWT in the H1 wetland at 12:45 P.M., 23 June 1999.

[30] Figure 4 illustrates RWT photolysis rates over a 15-hour period, reaching a maximum between 12:30 and 1:00 P.M. The average photolysis rate coefficient in the main channel ($k = 9.93 \times 10^{-8}$ s^{-1}) represents both light and dark cycles by distributing the maximum photolysis rate constant over a 24-hour period. The average photolysis rate coefficient in the storage zone ($k_{stor} = 1.01 \times 10^{-8}$ s^{-1}) was nearly an order of magnitude less than calculated for direct sunlight conditions. *Suijlen and Buyse* [1994] reported similar rates (averaging 2.77×10^{-7} s^{-1}) in a long-term tracer test in the Loosdrecht Lakes located in the Netherlands. The k rate exponentially decays as z_{mix} increases the amount of background light-attenuating constituents (S_λ), and decreased 46% for depths (z_{mix}) in the wetlands ranging from 0.5 to 1.0 m. The z_{mix} term had negligible influence on k_{stor}, because obstruction of sunlight intensity due to shading is much greater than from the overlaying water.

4.2.2. Sorption

[31] The $K_{d,sed}$ value of 1.17×10^{-6} L μg^{-1} was calculated from the Freundlich isotherm for sorption of RWT to C1 sediments (Figure 5) as described by *Keefe* [2001]. Generally, sediment samples were collected, dried at 90°C, and passed through a 2 mm sieve. Amber polyethylene bottles were filled with 50 g of sediment and 50 mL of a RWT solution ranging from 1 to 1000 μg L^{-1}. Each point was prepared in triplicate and agitated for 3 days to achieve equilibrium. Sediment and solution phases were separated by centrifugation and an aliquot was removed to obtain the dissolved concentration. Similar methods were used to perform isotherm experiments for RWT and soft-stem and Onley's bulrush; however, the $K_{d,veg}$ represents both RWT diffusion into the plant cells and sorption. The $K_{d,veg}$ value (1.26×10^{-6} L μg^{-1}) is an average of measured partition coefficients for soft-stem bulrush (1.38×10^{-6} L μg^{-1}) and Olney's bulrush (1.14×10^{-6} L μg^{-1}) in the Hayfield effluent (Figure 5).

[32] The $K_{d,det}$ value was determined from the product of the organic carbon fraction (f_{oc}) and an organic carbon distribution coefficient, K_{oc} ($K_d = f_{oc}K_{oc}$). *Sabatini and Austin* [1991] reported K_{oc} values ranging from 1.70 to 3.70×10^{-6} L μg^{-1} for RWT; an average K_{oc} of 2.70×10^{-6} L μg^{-1} was used in this application. The measured K_{oc} of the C1 sediments was 1.46×10^{-5} L μg^{-1} ($f_{oc} = 0.08$), an order of magnitude higher than reported by *Sabatini and Austin* [1991]. *Rutherford et al.* [1992] measured an f_{oc} value of 0.53 for muck and 0.57 for peat, and the average was assumed to represent the f_{oc} of detritus. Similar results were reported for treatment wetland dissolved organic matter with f_{oc} values of 0.56 and 0.54 for the colloidal and hydrophobic acid fractions [*Barber et al.*, 2001]. *Lin et*

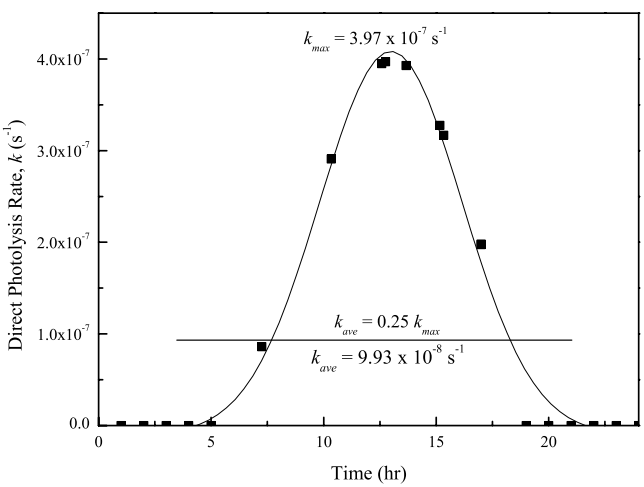

Figure 4. Diurnal photolysis rate distribution for RWT in the Hayfield 1 wetland, 23 June 1999.

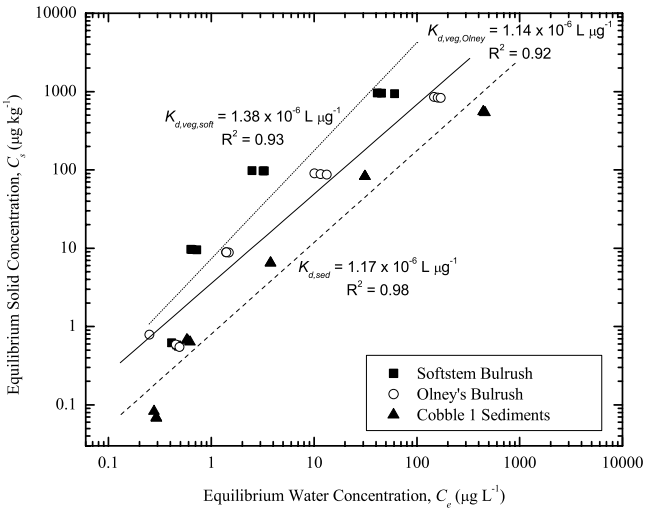

Figure 5. RWT sorption isotherm for soft-stem bulrush, Olney's bulrush, and Cobble 1 sediments. Legend is $K_{d,veg,soft}$, soft-stem bulrush–water distribution coefficient; $K_{d,veg,Olney}$, Olney's bulrush–water distribution coefficient; $K_{d,sed}$, sediment-water distribution coefficient.

al. [2003] showed wetland plant detritus exhibited high sorption capacities for RWT and that sorption was mainly irreversible for a 12 day desorption experiment; no K_{oc} or f_{oc} values were reported for wetland detritus. *Rutherford et al.* [1992] measured an f_{oc} value of 0.44 for cellulose which generates a calculated $K_{d,veg}$ value of 1.19×10^{-6} L μg^{-1}, 95% of the measured $K_{d,veg}$ value. The total sorptive material in each wetland was divided into 40% sediment (f_{sed} = 0.4), 20% vegetation (f_{veg} = 0.2), and 40% detritus (f_{det} = 0.4) based on field observations. A composite K_d value of 1.32×10^{-6} L μg^{-1} (equation (6)) was used to describe main channel RWT sorption for all three wetland sites.

4.2.3. Reactive Simulations

[33] Figure 6a depicts model simulations of RWT photolysis and sorption in the H1 wetland. The photolysis-only simulation had a peak concentration 34% greater than field data. Invoking main channel and storage zone RWT sorption in addition to photolysis resulted in an improved solution that demonstrated excellent agreement with field concentrations, with a difference in mass recovery of 0.03% and in HRT of 0.74%. The standard deviations of the ρ and k_{sorp} terms were less than 6% of mean values, while the $k_{sorp,stor}$ parameter standard deviation was 15% of the mean value. On the basis of OTIS simulation results, RWT reactive losses in the H1 wetland totaled 21%, with 10% attributed to photolytic degradation and 11% resulting from sorption processes. Photolysis and sorption reactions in the main channel and storage zone of the H1 wetland resulted in the greatest overall reactive losses of the three wetland configurations.

[34] Figure 6b depicts RWT photolysis and sorption in the C1 wetland. The photolysis-only simulation overestimated the tracer peak by 22% and did not replicate concentrations in the falling limb and tail regions of the field tracer response curve. When sorption was incorporated, the simulation demonstrated agreement with field concentrations with a difference in mass recovery and HRT of 0.13% and 5.3%, respectively. Transient storage in C1 did not influence the conservative transport simulation (Table 3) and therefore was not considered in the RWT simulations. The standard deviations of the ρ and k_{sorp} parameters were 56% and 61% of mean values, the largest uncertainty associated with any of the data sets. The leaky nature of the C1 wetland dominated the hydraulics and influenced the estimation of both reactive and conservative parameters. Simulation results indicated a 4.8% RWT reactive loss with 1.2% resulting from photolysis and 3.6% from sorption.

[35] The photolysis-only simulation for the C2 wetland (Figure 6c) had a 34% greater peak concentration than the field tracer response curve and underestimated the tail after 75 hours. Using both photolysis and main channel sorption resulted in good agreement with field concentrations, and indicated RWT sorption in the storage zone did not influence concentrations. The standard deviations of the ρ and k_{sorp} parameters were 11% of the mean values. The simulation using both photolysis and main channel sorption yielded a difference in mass recovery of 0.25% and in HRT of 11.5% from field concentrations. RWT underwent the least amount of reactive loss in the C2 wetland (1.6%), with 0.75% of the mass loss attributed to photolysis and 0.88% to sorption.

5. Discussion

[36] Wetland flows were characterized by low velocities relative to open channel hydraulics resulting in increased reaction times and transient storage interactions. Transient storage areas can have different reactions and rates relative to main channel conditions [*Bencala*, 1983; *Valett et al.*, 1996; *Harvey and Fuller*, 1998]. The D parameters for H1 and C1 (9.97×10^{-3} m^2 s^{-1}; 2.13×10^{-2} m^2 s^{-1}) fall within the range of dispersion coefficients ($1.69 \times 10^{-2} \pm 9.76 \times 10^{-3}$ m^2 s^{-1}) reported by *Kadlec* [1994] for a similarly designed constructed wetland on the Des Plaines River (205 m length; 0.6 m average depth; and 6.5 cm d^{-1} HLR). Wetland flows at Tres Rios are classified as laminar (R_e < 600) and subcritical (F_r < 1) with transitional flow between a PFR and CSTR (0.1 < P_e < 10).

[37] Increased mixing ($A/A_{design} \approx 69\%$; emergent vegetation ≈ 30%) and transient storage exchange influenced solute transport and RWT removal in the H1 wetland. The H1 exchange coefficient ($\alpha = 9.00 \times 10^{-7}$ s^{-1}) was several orders of magnitude less than exchange coefficients reported for reaches of the Willamette River ($1.85 \times 10^{-4} \pm 1.48 \times 10^{-4}$ s^{-1}), a large river system [*Laenen and Bencala*, 2001] with average flows (8.79×10^6 m^3 d^{-1}) considerably larger than the H1 wetland (1.89×10^3 m^3 d^{-1}). The compacted nature of the underlying soils curtailed permanent mass and flow losses to the subsurface and promoted reactive RWT loss (21%) in the main channel and storage zones. Transient storage occurred primarily in stagnant water areas containing emergent vegetation and detritus, increasing contact time with available sorption sites. The average solute travel time associated with the storage zone was short relative to the main channel, providing sufficient time for photolysis reactions to occur in open-water areas.

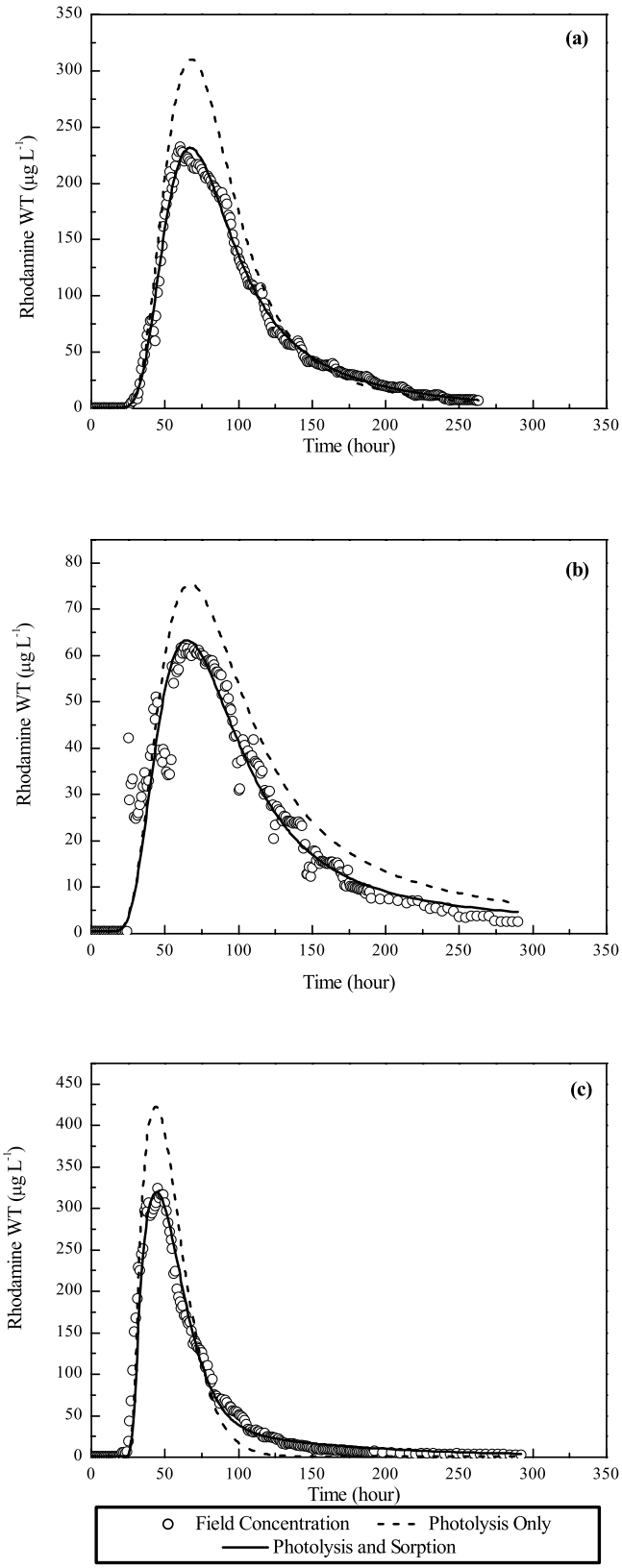

Figure 6. RWT tracer test field data, and photolysis and sorption model simulations for the (a) Hayfield 1, (b) Cobble 1, and (c) Cobble 2 wetlands, 24 June through 6 July 1999.

[38] In contrast, the leaky nature of the C1 wetland dominated hydraulics in the main channel where advection and dispersion governed conservative solute transport. A minimal influence of transient storage was observed on solute transport and travel time. The delay of water velocities associated with the large flow and solute losses resulted in a 27% longer field HRT than volumetric nHRT value. The reactive RWT losses at the C1 outlet location (4.8%) were <25% of the reactive losses measured in the H1 wetland. The majority of mass loss occurred via groundwater seepage, therefore assessing the functionality of the C1 wetland may be better accomplished by examining concentration changes in the subsurface rather than at the outlet location. Investigation of multilevel subsurface samplers (MLS), placed along the length of the wetland during a subsequent coupled bromide and RWT tracer test in the C1 wetland, concluded that at the outlet MLS, RWT average HRT values were longer than bromide HRT values by 37% just below the sediment/water interface, 16% at a depth of 4.6 m, and 20% at a depth of 6.1 m. The delay of the RWT plume relative to the conservative bromide tracer suggests increased contact time for subsurface sorption reactions to occur.

[39] The islands in the C2 wetland were parallel to the direction of flow, which resulted in channelization of the solute plume and nominal mixing, characterized by increased flow velocities and consequently a very short HRT. The C2 transient storage exchange rate of 2.78×10^{-5} s^{-1} was comparable to those reported for streamflow conditions (1.2 to 4.8×10^{-5} s^{-1}) by *Chapra and Wilcock* [2000] and *McKnight et al.* [2001]. The limited contact time of the solute plume in the wetland resulted in minimal RWT removal (1.6%). A shallow zone immediately upstream of the outlet structure had less emergent vegetation cover and provided a large, shallow area fully exposed to incident solar radiation that may have increased photolysis reactions despite the short HRT. The median travel time calculations did not provide a good indicator of the influence of transient storage on solute travel time due to the channel flow and two-dimensional flow characteristics of the wetland.

[40] The conservative transport parameters provide insight into the effects of wetland configuration and governing hydraulic profiles on solute transport and transient storage. For example, simulations of the relatively impermeable H1 wetland with deep zones situated perpendicular to flow demonstrated increased mixing and transient storage interactions (F_{mean} = 13.9%; F_{med} = 6.5%) relative to the Cobble wetlands. The significantly leaky C1 wetland was governed by advection and dispersion only, with the large flow losses overriding any transient storage interactions. The islands situated parallel to the flow direction in the C2 wetland resulted in channel flow characterized by average flow velocities 2.6–2.9 times faster than the H1 and C1 wetlands, a transient storage exchange rate comparable to streamflow conditions, and an A parameter 22% of the design value.

[41] The coupled field experiments presented here demonstrate the nonconservative nature of RWT as a hydraulic tracer. Despite the mass loss and retention by sorption, the RWT HRT values were only 3.8–10% longer than bromide values, showing general agreement between the two tracers for estimating average detention times. *Lin et al.* [2003] conducted a coupled tracer test in the Prado wetlands and also found general agreement with bromide and RWT HRT

values (53–55 hours) and similar tracer mass losses (15% for bromide; 41% for RWT) in a pilot experiment (two serially connected wetlands, 8.9 ha each, with an average flow of 18.1×10^3 m^3 d^{-1}).

[42] For this investigation, RWT reactive losses are considered as a sum of the first-order photolysis reactions and sorption loss. The RWT photolysis term is based on direct photolysis, while in the field indirect photolytic reactions can be induced by dissolved organic matter [*Schwarzenbach et al.*, 1993] and contribute to overall first-order losses. The sorption term is more complex [*Bencala et al.*, 1983], and any retardation of the RWT curve is attributed to a bulk sorptive removal. On the timescale of the tracer test, prolonged physical entrapment of RWT can occur due to diffusion into vegetation cell walls as well as largely irreversible sorption interactions with the surface of vegetation, sediments, detritus, and biofilms.

6. Conclusions

[43] This research addresses the challenges of using numerical models to simulate complex environmental systems. The one-dimensional flow with transient storage OTIS model is suitable for constructed wetlands with hydraulic profiles similar to the H1 wetland. Extreme hydraulic conditions, including significant leakage and channel flow, limit transient storage evaluation. The approach outlined here provides an advanced technique to perform forward dynamic modeling scenarios by establishing the hydraulics and subsequently investigating removal pathways. The methodology used to estimate first-order photolysis rates from field and laboratory measurements and chemical theory demonstrates a technique based on fundamental principles. A consistent approach was used to estimate sorption parameters in an attempt to minimize error and variability. However, because of the complexity of the sorption process, results are highly variable.

[44] The coupling of reactive and conservative transport provides insight into the influence of wetland design on photolysis and sorption. For example, the H1 wetland is characterized by mixing, transient storage interactions, and the most reactive mass loss overall. In contrast, channel flow, short retention time, and the least reactive mass loss occurred in the C2 wetland. Significantly leaky wetlands may also offer beneficial treatment alternatives by extended subsurface contact and residence times common in soil-aquifer treatment systems. The effects of mass loading and hydraulic profiles on the fate of other reactive solutes can be explored using removal rates calculated from routine monitoring data or chemical theory for other first-order removal processes such as volatilization.

[45] **Acknowledgments.** This work was carried out with support from the United States Bureau of Reclamation (USBR) in Denver, Colorado. The authors wish to thank Eric Stiles, Will Doyle, Kate Cambell, Greg Brown, Ron Elkins, Wes Camfield, Paul Kinshilla, and the City of Phoenix Wastewater Monitoring Laboratory for oversight, field support, and laboratory assistance. Anonymous reviewers have offered constructive comments to clarify and improve the manuscript. The use of firm, trade, and brand names in this report is for identification purposes only and does not constitute endorsement by the U.S. Geological Survey.

References

Barber, L. B., J. A. Leenheer, T. I. Noyes, and E. A. Stiles (2001), Nature and transformation of dissolved organic matter in treatment wetlands, *Environ. Sci. Technol.*, *35*, 4805–4816.

Bencala, K. E. (1983), Simulation of solute transport in a mountain pool-and-riffle stream with a kinetic mass transfer model for sorption, *Water Resour. Res.*, *19*, 732–738.

Bencala, K. E., and R. A. Walters (1983), Simulation of solute transport in a mountain pool-and-riffle stream: A transient storage model, *Water Resour. Res.*, *19*, 718–724.

Bencala, K. E., R. E. Rathbun, A. P. Jackman, V. C. Kennedy, G. W. Zellweger, and R. J. Avanzino (1983), Rhodamine WT dye losses in a mountain stream environment, *Water Resour. Bull.*, *19*, 943–950.

Buchberger, S. G., and G. B. Shaw (1995), An approach toward rational design of constructed wetlands for wastewater treatment, *Ecol. Eng.*, *4*, 249–275.

Carleton, J. N. (2002), Damköhler number distributions and constituent removal in treatment wetlands, *Ecol. Eng.*, *19*, 233–248.

Chapra, S. C. (1997), *Surface Water-Quality Modeling*, 844 pp., McGraw-Hill, New York.

Chapra, S. C., and R. J. Wilcock (2000), Transient storage and gas transfer in lowland streams, *J. Environ. Eng.*, *126*, 708–712.

Chaudhry, M. H. (1993), *Open-Channel Flow*, 483 pp., Prentice-Hall, Upper Saddle River, N. J.

Feng, K. E., and F. J. Molz (1997), A 2-D, diffusion-based, wetland flow model, *J. Hydrol.*, *196*, 230–250.

Fernald, A. G., P. J. Wigington Jr., and D. H. Landers (2001), Transient storage and hyporheic flow along the Willamette River, Oregon: Field measurements and model estimates, *Water Resour. Res.*, *37*, 1681–1694.

Getsinger, K. D., E. G. Turner, J. D. Madsen, and M. D. Netherland (1997), Restoring native vegetation in a Eurasian water milfoil-dominated plant community using the herbicide triclopyr, *Reg. Rivers Res. Manage.*, *13*, 357–375.

Guardo, M., and R. S. Tomasello (1995), Hydrodynamic simulations of a constructed wetland in South Florida, *Water Resour. Bull.*, *31*, 687–702.

Harvey, J. W., and C. C. Fuller (1998), Effect of enhanced manganese oxidation in the hyporheic zone on basin-scale geochemical mass balance, *Water Resour. Res.*, *34*, 623–636.

Kadlec, R. H. (1994), Detention and mixing in free water wetlands, *Ecol. Eng.*, *3*, 345–380.

Kadlec, R. H. (2000), The inadequacy of first-order treatment wetland models, *Ecol. Eng.*, *15*, 105–119.

Kadlec, R. H., and R. L. Knight (1996), *Treatment Wetlands*, 893 pp., Lewis Publ., Boca Raton, Fla.

Kasnavia, T., D. Vu, and D. A. Sabatini (1999), Fluorescent dye and media properties affecting sorption and tracer selection, *Ground Water*, *37*, 376–381.

Keefe, S. H. (2001), Modeling transport and fate of organic compounds in constructed wetlands, M.S. thesis, 142 pp., Univ. of Colo., Boulder.

Laenen, A., and K. E. Bencala (2001), Transient storage assessments of dye-tracer injections in rivers of the Willamette basin, Oregon, *J. Am. Water Resour. Assoc.*, *37*, 367–377.

Levenspiel, O. (1972), *Chemical Reaction Engineering*, 578 pp., John Wiley, Hoboken, N. J.

Lin, A. Y., J. F. Debroux, J. A. Cunningham, and M. Reinhard (2003), Comparison of rhodamine WT and bromide in the determination of hydraulic characteristics of constructed wetlands, *Ecol. Eng.*, *20*, 75–88.

McKnight, D. M., B. A. Kimball, and R. L. Runkel (2001), pH dependence of iron photoreduction in a rocky mountain stream affected by acid mine drainage, *Hydrol. Processes*, *15*, 1979–1992.

Morrice, J. A., H. M. Valett, C. N. Dahm, and M. E. Campana (1997), Alluvial characteristics, groundwater-surface water exchange and hydrological retention in headwater streams, *Hydrol. Processes*, *11*, 253–267.

Pfaff, J. D., D. P. Hautman, and D. J. Munch (1997), Method 300.1 Determination of inorganic anions in drinking water by ion chromatography, Rev. 1.0, 40 pp., U.S. Environ. Prot. Agency, Cincinnati, Ohio.

Ptak, T., and G. Schmid (1996), Dual-tracer transport experiments in a physically and chemically heterogeneous porous aquifer: Effective transport parameters and spatial variability, *J. Hydrol.*, *183*, 117–138.

Rash, J. K., and S. K. Liehr (1999), Flow pattern analysis of constructed wetlands treating landfill leachate, *Water Sci. Technol.*, *40*, 309–315.

Runkel, R. L. (1998), One-dimensional transport with inflow and storage (OTIS): A solute transport model for streams and rivers, *U.S. Geol. Surv. Water Res. Invest. Rep.*, *98-4018*, 73 pp.

Runkel, R. L. (2002), A new metric for determining the importance of transient storage, *J. N. Am. Benthol. Soc.*, *21*, 529–543.

Runkel, R. L., and S. C. Chapra (1993), An efficient numerical solution of the transient storage equations for solute transport in small streams, *Water Resour. Res.*, *29*, 211–215.

Runkel, R. L., D. M. McKnight, and E. D. Andrews (1998), Analysis of transient storage subject to unsteady flow: Diel flow variation in an Antarctic stream, *J. N. Am. Benthol. Soc.*, *17*, 143–154.

Rutherford, D. W., C. T. Chiou, and D. E. Kile (1992), Influence of soil organic matter composition on the partition of organic compounds, *Environ. Sci. Technol.*, *26*, 336–340.

Sabatini, D. A., and T. A. Austin (1991), Characteristics of rhodamine WT and fluorescein as adsorbing ground-water tracers, *Ground Water*, *29*, 341–349.

Schwarzenbach, R. P., P. M. Gschwend, and D. M. Imboden (1993), The gas-liquid interface: Air-water exchange, in *Environmental Organic Chemistry*, chap. 10, pp. 215–241, John Wiley, Hoboken, N. J.

Smart, P. L., and I. M. S. Laidlaw (1977), An evaluation of some fluorescent dyes for water tracing, *Water Resour. Res.*, *13*, 15–33.

Somes, N. L. G., W. A. Bishop, and T. H. F. Wong (1999), Numerical simulation of wetland hydrodynamics, *Environ. Int.*, *25*, 773–779.

Stairs, D. B., and J. A. Moore (1994), Flow characteristics of constructed wetlands: Tracer studies of the hydraulic regime, in *Proceedings of the 4th International Conference on Wetland Systems for Water Pollution Control*, pp. 742–751, S. China Inst. for Environ. Stud., Guangzhou, China.

Stern, D. A., R. Khanbilvardi, J. C. Alair, and W. Richardson (2001), Description of flow through a natural wetland using dye tracer tests, *Ecol. Eng.*, *18*, 173–184.

Suijlen, J. M., and J. J. Buyse (1994), Potentials of photolytic rhodamine WT as a large-scale water tracer assessed in a long-term experiment in the Loosdrecht lakes, *Limnol. Oceanogr.*, *39*, 1411–1423.

Sutton, D. J., Z. J. Kabala, A. Francisco, and D. Vasudevan (2001), Limitations and potential of commercially available rhodamine WT as a groundwater tracer, *Water Resour. Res.*, *37*, 1641–1656.

Tai, D. Y., and R. E. Rathbun (1988), Photolysis of rhodamine-WT dye, *Chemosphere*, *17*, 559–573.

Tisdale, T. S., and P. D. Scarlatos (1989), Simulation of wetland flow dynamics, in *Water*: *Laws and Management*, pp. 9A-15–9A-23, Am. Water Resour. Assoc., Bethesda, Md.

U.S. Environmental Protection Agency (1985), Rates, constants, and kinetics formulations in surface water quality modeling, 2nd ed., *EPA 600/3-85-040*, 455 pp., Off. of Res. and Dev., Environ. Res. Lab., Athens, Ga., June.

U.S. Environmental Protection Agency (1998), Fate, transport and transformation test guidelines OPPTS 835.2210: Direct photolysis rate in water by sunlight, *EPA 712-C-98-060*, 35 pp., Off. of Prev., Pestic., and Toxic Subst., Washington, D. C., Jan.

Valett, H. M., J. A. Morrice, C. N. Dahm, and M. E. Campana (1996), Parent lithology, surface-groundwater exchange, and nitrate retention in headwater streams, *Limnol. Oceanogr.*, *41*, 333–345.

Vasudevan, D., R. L. Fimmen, and A. B. Francisco (2001), Tracer-grade rhodamine WT: Structure of constituent isomers and their sorption behavior, *Environ. Sci. Technol.*, *35*, 4089–4096.

Wass, R. D. (1997), Tres Rios demonstration constructed wetland project: 1996/1997 operation and water quality report, 34 pp., Water Serv. Dep., City of Phoenix, Ariz., Sept.

Wass, Gerke and Associates, Inc. (2001), Status report to the 1998 research plan for the Tres Rios demonstration constructed wetland project, 67 pp., Tempe, Ariz., Aug.

Werner, T. M., and R. H. Kadlec (2000), Wetland residence time distribution modeling, *Ecol. Eng.*, *15*, 77–90.

Whitmer, S. B. (1998), Hydraulic characterization of treatment wetlands to improve design modeling and treatment efficiency, M.S. thesis, 76 pp., Ariz. State Univ., Tempe.

Zepp, R. G., and D. M. Cline (1977), Rates of direct photolysis in aquatic environments, *Environ. Sci. Technol.*, *11*, 359–366.

L. B. Barber and S. H. Keefe, U.S. Geological Survey, 3215 Marine Street, Room E127, Boulder, CO 80303, USA. (shkeefe@usgs.gov)

D. M. McKnight, Department of Civil, Environmental, and Architectural Engineering, 450 UCB, University of Colorado, Boulder, Boulder, CO 80303, USA.

R. L. Runkel, Denver Federal Center, P.O. Box 25046, Mail Stop 415, Lakewood, CO 80225, USA.

J. N. Ryan, Department of Civil, Environmental, and Architectural Engineering, 428 UCB, University of Colorado, Boulder, Boulder, CO 80303, USA.

R. D. Wass, Wass, Gerke and Associates, Inc., 1426 N. Sunset Drive, Tempe, AZ 85281, USA.